crops

MDPI

Article

Joint Modeling of Grain Yield and Root Lodging in Maize Using Multi-Output Neural Network and Machine Learning Models Under Defined Environmental Conditions

Dušan Dunđerski [1,*], Božana Purar [1], Anja Đurić [1], Maja Tanasković [2], Dušan Stanisavljević [1] and Goran Bekavac [1]

[1] Institute of Field and Vegetable Crops, 21101 Novi Sad, Serbia
[2] The Agricultural Institute of Slovenia, 1000 Ljubljana, Slovenia
* Correspondence: dusan.dundjerski@nsseme.com

Abstract

We evaluated a multi-output neural network framework for jointly analyzing maize grain yield (GY) and root lodging percentage (LP) using above-ground morphological traits measured under defined environmental conditions. To address model robustness, the multi-output neural network was compared with linear regression, elastic net, random forest, and XGBoost using repeated five-fold cross-validation, an 80/20 holdout split, and independent year-wise validation. Under repeated cross-validation, XGBoost provided the strongest average predictive performance for both traits, with R^2 values of 0.57 for GY and 0.67 for LP. The multi-output neural network showed moderate performance, with R^2 values of 0.49 for GY and 0.57 for LP. Final holdout performance for the neural network for GY and LP was R^2 = 0.64 and R^2 = 0.92, respectively. Year-wise validation showed weak temporal transferability because the two seasons differed not only in environmental conditions, but also in lodging mechanism. Repeated permutation importance identified ear width (EW), kernel row number (RNE), thousand kernel mass (KM1000), and kernel number per ear (KNE) as important predictors of GY, while LP prediction was most strongly associated with internode major diameter (IDmajor), ear length (EL), and the number of green leaves (NGL). Across both permutation importance and SHAP, only RNE and NGL were consistently shared between GY and LP. Supplementary ALE diagnostics indicated that RNE showed increasing model-estimated effects for both predicted GY and LP, whereas NGL showed a positive association with predicted GY but a decreasing or nonlinear association with predicted LP. These results show that joint modeling can support exploratory trait interpretation, but the predictive relationships remain environment-specific and should not be interpreted as causal or broadly transferable without further multi-environment validation.

Keywords: grain yield; lodging; maize; machine learning; permutation feature importance

Academic Editor: Shichao Jin

Received: 11 April 2026
Revised: 26 May 2026
Accepted: 17 June 2026
Published: 22 June 2026

1. Introduction

Maize is one of the most important crops in the world and plays a crucial role in global agriculture and food systems. It is widely used as staple food for humans, and approximately 85% of maize is utilized for animal feed and bioethanol production [1]. Nevertheless, maize production is increasingly challenged by a range of stresses, one of the most significant being lodging. Lodging causes grain yield (GY) and quality reduction

and increases drying costs [2]. Stalk lodging occurs when the bending moments along the stalk, caused by a combination of external factors (e.g., wind) and self-loading (the weight of individual plant organs), exceed the resistance provided by the stalk [3]. Annual grain yield losses due to stalk lodging represent a severe problem that hampers the efficiency of maize production. According to expert estimates, stalk lodging reduces global maize grain yield by 5–25% [4].

Root lodging is a common phenomenon in maize production, occurring when the plant tilts under the influence of intense winds, and the base of the stalk is no longer vertical to the soil surface, preventing it from straightening after the wind subsides [5]. Root lodging happens when the plant is not sufficiently anchored in the soil to withstand storm winds and heavy rains. This type of lodging damages the root system, alters the normal upright position of the plant, reduces photosynthetic activity, and results in yield reduction. If lodging occurs in the later stages of growth, the ears may lie on the ground, increasing the risk of ear diseases and degrading grain quality. Naturally, lodging also reduces harvest efficiency [6]. The risk of root lodging can arise throughout the whole maize growth cycle [7].

As there are tradeoffs between yield formation and lodging resistance during the entire maize growth period, it is crucial to reduce lodging risk as well as increase GY by optimizing above-ground plant traits [8]. Insights into specific traits that should be optimized can be gained by developing predictive models for both GY and lodging simultaneously within the same analytical pipeline.

Above-ground plant traits play a crucial role in understanding lodging as abiotic stress [9,10]. Lodging stress is determined by plant height (PH), ear height (EH), internode length (IL) [11,12], the ratio of rind thickness to diameter [13] and leaf area index [14]. It is also influenced by internode dry weight (DW), dry weight per unit length (DWUL), and ear traits, such as the length of the ear (EL), number of kernels per ear (KNE) and kernel row number per ear (RNE), which together determine ear weight [15]. In cereals, it is well known that the weight of the ear/spike is an important trait determining their tolerance to lodging [16]. Ear weight in maize increases steadily from the R1 stage, leading to a reduction in the mechanical strength and dry mass of the stalk due to the transport of non-structural carbohydrates to the ear, which also raises the plant's center of gravity [17]. According to Xue et al. (2020) [11], maize lodging tolerance must consider not only wind speed, leaf area, ear height, and the mechanical properties of internodes, but also ear weight. Shoot fresh weight, dry weight per length of the third internode, and upper nodal root determine maize lodging [18].

Above-ground plant traits play a crucial role in yield prediction. The number of green leaves (NGL), PH, EH, EH/PH, DW and EL are significantly important traits in the estimation of maize GY and explain over 60% in GY [15]. Plant height and associated traits, such as EH, node number, and IL, correlate closely with biomass and GY, as well as lodging tolerance [19]. The number of plants per m^2 and PH are the most important explanatory traits for rice yield per m^2, with an explained variation of 32.5% and 20.6%, respectively. Rice yield was directly affected by panicle numbers and panicle weight [20].

Developing data-driven analytical models has become increasingly common in modern agriculture to support the interpretation of complex trait relationships and management decisions within defined production environments. This approach allows for more precise management of resources, leading to increased efficiency and higher crop yield [21,22]. Developing models using plant traits is also important in breeding, as we can determine the most important traits specific for each breeding program [23,24]. Earlier predictions were made for grain yield [25,26] and lodging [27,28]. Although GY and lodging have often been modeled separately, both traits can be influenced by overlapping morphological

and structural plant characteristics. Simultaneous modeling may therefore provide an exploratory framework for identifying predictors that are associated with both productivity and lodging susceptibility. However, the value of a multi-output approach should not be assumed from model complexity alone, but should be evaluated by comparing predictive performance, validation stability, and interpretability against alternative models.

The objectives of this study were to (1) evaluate whether a multi-output neural network can jointly model maize GY and root LP under defined environmental conditions; (2) compare its predictive performance with linear regression, elastic net, random forest, and XGBoost baselines; (3) assess robustness using repeated cross-validation, confidence intervals, hyperparameter sensitivity, and year-wise validation; and (4) identify aboveground plant traits consistently associated with both GY and root lodging. Because the dataset was restricted to one location, two seasons, and a specific set of treatments, the analysis was intended as an exploratory, environment-specific modeling framework rather than a broadly transferable prediction model.

2. Materials and Methods

2.1. Experimental Design and Description of Factors and Treatments

The trial was organized as a split-plot design with four replications, where the ethephon rates (ERs) represented the main factor with four treatments (0, 280, 560, and 840 g/ha), and sowing densities (SDs) the sub-factor with three treatments (65,000, 75,000 and 85,000 seeds/ha). Ethephon was applied when the hybrids reached the V8 growth stage [29,30]. The hybrids used in the experiment were NS3022 and NS4000. Ethephon treatments were applied using a CO_2-pressurized plot sprayer equipped with TeeJet XR 11,003 flat-fan nozzles mounted on a 3 m boom (TeeJet Technologies, Glendale Heights, IL, USA).

2.2. Crop Management

Nitrogen fertilization was based on a five-year preliminary trial aimed at finding the optimal nitrogen dose for achieving the highest maize yield under the agroecological conditions of the experiment site. On 20 December 2020 and 18 November 2021, 860 kg ha^{-1} and 635 kg/ha of mineral fertilizer (NPK formulation 8:15:15) was applied, respectively. This amount of fertilizer, based on the basic agrochemical analysis of the soil, provided the necessary amounts of phosphorus and potassium for the planned maize yield of 10 t ha^{-1}, considering the known nutrient removal rates per unit of yield.

Winter plowing was performed on 21 December 2020 and 19 November 2021. In the spring, on 17 April 2021 and 6 April 2022, urea mineral fertilizer was applied at rates of 184 and 218 kg/ha, respectively, followed by pre-sowing soil preparation performed on the same day. These amounts of mineral fertilizer provided the total nitrogen input for both years (according to the preliminary trial, 150 kg/ha). Planting was carried out on 26 April 2021 and 21 April 2022, using a pneumatic seeder of the brand "Nodet" with four sections. Between row cultivation, herbicide and insecticide treatments, and manual weed removal were performed as part of the crop care measures in later growth stages.

2.3. Analyzed Traits

2.3.1. Plant Height, Ear Height, Ratio of Ear Height to Plant Height, and Number of Green Leaves

These traits were analyzed in two central rows, with five representative plants for each variant within each replication, when the plants were in the R1 growth stage. Plant height (PH) was measured using a measuring tape, from the soil surface to the tip of the tassel, while EH was measured from the soil surface to the node carrying the ear. The ratio

of EH to PH was obtained by dividing EH by PH. The NGL was recorded simultaneously with height measurements, and a leaf was considered green if it had at least 50% green surface [31].

2.3.2. Leaf Length and Width, Angle of the Leaf Above the Ear, and Plant Width

These traits were analyzed when maize reached the R3 growth stage, 18–22 days after silking [32]. From the central two rows, three plants were selected for each variant within each replication. Measurements of leaf length (LL) and leaf width (LW) were taken on the leaf above the ear. The leaf angle (LA) was measured on the leaf above the ear using a mobile phone with the Clinometer app [33], at the point where the leaf base and the stalk meet. Leaf length was measured using a digital laser rangefinder. LW was measured with a digital caliper up to the vein that divides the leaf into two parts, at the widest part of the leaf. The recorded width was then multiplied by two to obtain the actual LW. Plant width (PW) [31] was obtained based on the sine theorem, multiplying the sine of the LA above the ear by its LL. This provided the width of the plant on one side of the stalk. Multiplying by two gave the PW of the entire plant.

2.3.3. Third Internode Traits

Three plants per variant in each replication, selected from rows 1 and 4, were used to determine these traits. Sampling was performed approximately 45 days after silking [34]. The stalks were cut using a battery-powered angle grinder, first above and then below the third internode above the ground. The cutting site was at the nodes that delimit the third internode. Before cutting, leaves were removed from the plant, ensuring that the internode showed no external signs of damage. The length of the internode (IL) was measured from node to node using a measuring tape, and then the fresh weight was measured. A cross-section of one-half of each internode was then scanned following the methodology described by [34]. Each photograph was processed using the Fiji/ImageJ software version 1.54f. The methodology by [15] was used to determine the diameter of the minimum axes (ID minor), the diameter of the maximum axes (ID major), the thickness of the rind (RT) and the cross-sectional area (CSA) of the internode. After measuring the fresh weight and scanning the internodes, they were dried at 100 °C to the constant weight. The dry weight per unit length (DWUL) of the internode was obtained by dividing the DW with the IL of the internode. The area moment of inertia and section modulus are terms that are copied from engineering. The area moment of inertia describes how the building material of the cross-section is distributed [35]. Section modulus quantifies the overall bending strength of a beam's cross-section and is calculated as the area moment of inertia divided by the perpendicular distance from the neutral bending axis to the outermost point of the section. It is assumed that the cross-section of the maize stalk is a hollow ellipse [35]. Rather than using the standard area moment of inertia and section modulus, the ellipse-based area moment of inertia of the rind along the minor diameter (eMOI) (Equation (1)) and the ellipse-based section modulus along the minor diameter (eSM) (Equation (2)) are adopted here as the more appropriate metrics.

$$\text{eMOI} = \pi/4[Rr^3 - (R - t)(r - t)^3]\ (\text{cm}^4) \quad (1)$$

$$\text{eSM} = \{\pi/4[Rr^3 - (R - t)(r - t)^3]\}/r\ (\text{cm}^3) \quad (2)$$

2.3.4. Lodging Percentage

The LP was analyzed in the central two rows of each variant in each replication simultaneously with determining the total number of plants in the same two rows, just before harvest. A plant was classified as lodged when its stalk formed an angle of less than

45° with the ground (root lodging) or when structural failure occurred below the ear (stalk lodging) [36].

2.3.5. Ear Traits and Grain Yield

To determine ear traits, 10 ears were taken from 10 plants of each variant per replication just before harvest. Ear length (EL) and width (EW) were measured according to [37] guidelines, with EL measured with a ruler and EW with a digital caliper. The length of the non-grain portion of the ear was measured using a digital caliper. The length of the ear (EL), excluding the non-grain portion, was calculated by subtracting the length of the barren portion from the total ear length. The kernel row number on the ear (RNE) was also determined. Subsequently, the fresh weight of the ears was measured, followed by the ear shelling process. The fresh weight of all kernels was measured on an analytical scale, and the number of kernels per ear (KNE) was counted using an electronic kernel counter. After measuring the fresh weight and the number of kernels, 100 g of kernels were dried at 105 °C to constant weight, at which point the difference between the initial mass and the dry mass of the kernels represented the moisture content (GM). Grain yield (GY) was determined mechanically by harvesting maize with a Wintersteiger Split combine (WINTERSTEIGER, Ried im Innkreis, Austria) and was adjusted to 14% moisture. The GY obtained was subsequently converted to a yield of dry grain expressed in t ha^{-1}.

2.4. Statistical Analysis

The statistical analysis was conducted using the R programming language version 4.3.2. We loaded the raw dataset from a Microsoft Excel file, ensuring that all columns regarding predictors and dependent variables were present. Missing values were identified using the 'sapply' function. Missing values within predictor variables were imputed using k-nearest neighbors (k-NN) imputation via the 'kNN' function from the 'VIM' package. According to [38], the k-NN imputation method demonstrated strong performance in managing missing values and achieved predictive accuracy comparable to analyses conducted on the complete dataset. Outliers were detected in the training data using the interquartile range (IQR) method. Observations with predictor values outside three times the IQR from the first and third quartiles ("far out" outliers) were considered outliers and removed to reduce their impact on model training [39]. Predictor variables were standardized using z-score normalization with the 'preProcess' function, ensuring that all features contributed equally to the model training process.

The final modeling dataset contained 192 observations and 23 predictor variables. Five predictive approaches were evaluated: linear regression, elastic net regression, random forest, XGBoost, and a multi-output neural network. Linear regression, elastic net, random forest, and XGBoost were trained separately for GY and LP. The multi-output neural network was trained to predict both outcomes simultaneously. The multi-output neural network consisted of four hidden layers with 128, 64, 32, and 16 neurons, respectively, using rectified linear unit activation functions. L2 regularization was applied to the dense layers. The Adam optimizer was used with a learning rate of 0.001 and a batch size of eight. The final neural network configuration was trained for 200 epochs. Hyperparameter sensitivity of the 80/20 neural network model was assessed by comparing alternative network depths and L2 regularization strengths using the same preprocessing, train–test split, target scale, optimizer, batch size, and number of epochs as the holdout neural network analysis. This analysis was used as a diagnostic check of model stability.

Model performance was evaluated using RMSE, MAE, and R^2. A single random 80/20 train–test split was first used as an initial holdout analysis to examine basic model fit. However, because single splits can be sensitive to the random allocation of observations, this

analysis was not used as the primary evidence of predictive reliability. Models' predictive reliability was evaluated using repeated five-fold cross-validation with 10 repeats, resulting in 50 validation runs. Mean values and 95% confidence intervals were calculated for each performance metric. Independent year-wise validation was then used as a stricter test of temporal transferability by training models on one year and testing them on the other.

Feature importance was evaluated using repeated permutation importance. For each predictor, the predictor values were permuted 300 times in the test set, and the increase in RMSE relative to the baseline prediction error was recorded. The mean increase in RMSE, 95% confidence intervals, and mean rank were calculated for each predictor. As an additional interpretability check, SHAP-style contribution values were calculated from the XGBoost models for GY and LP. Accumulated local effect (ALE) plots were generated as supplementary diagnostic plots for the highest-ranking predictors from the 80/20 multi-output neural network model.

2.5. Experimental Site and Defined Environmental Conditions

The experiment was conducted in 2021 and 2022 in Budisava, Vojvodina, Republic of Serbia (Table 1). The trial was set up on a 5964 m^2 plot belonging to a private producer. The soil type on the site is chernozem: class A–C (humus-accumulative soil), type—chernozem on loess and loess-like sediments, variety—calcareous, and moderately deep form (40–80 cm, according to A horizon depth) [40]. The agrochemical soil analysis is given in Table 1.

Table 1. Defined environmental conditions of experimental site.

	Parameter	2021 Season	2022 Season
Location	Latitude	45°17′22.4″ N	45°17′22.5″ N
	Longitude	20°01′41″ E	20°01′29″ E
	Altitude	76 m a.s.l.	76 m a.s.l.
	Place	Budisava, Vojvodina, Serbia	Budisava, Vojvodina, Serbia
Soil sampling	Sampling depth	0–30 cm	0–30 cm
	Sampling time	Autumn 2020	Autumn 2021
Soil properties	pH (KCl)	7.14 (neutral pH)	6.75 (neutral pH)
	pH (H_2O)	8.21	7.54
	$CaCO_3$ (%)	5.02 (high $CaCO_3$)	2.32 (medium $CaCO_3$)
	Humus (%)	2.40 (low content)	2.43 (low content)
	Total N (%)	0.12 (medium level)	0.12 (medium level)
	AL-P_2O_5 (mg/100 g)	12.85 (medium level)	24.67 (optimum level)
	AL-K_2O (mg/100 g)	24.94 (optimum level)	34.23 (high level)
Climate data source	Meteorological station	Rimski Šančevi	Rimski Šančevi
Climate reference	Long-term mean 1987–2016 (LTM)		
Autumn precipitation	Deviation from LTM	−1.43 mm	+91.57 mm
Autumn temperature	Deviation from LTM	+1.32 °C	+0.63 °C
Winter precipitation	Deviation from LTM	+25.73 mm	+9.73 mm
Winter temperature	Deviation from LTM	+3.49 °C	+2.26 °C
Spring precipitation	Deviation from LTM	−3.02 mm	−91.42 mm
Spring temperature	Deviation from LTM	−0.70 °C	−0.16 °C
Summer precipitation	Deviation from LTM	−66.02 mm	−49.02 mm
Summer temperature	Deviation from LTM	+2.01 °C	+2.54 °C
Maximum daily temperature	Range	32–41 °C	32–41 °C

The classification of the soil pH, $CaCO_3$, humus, total N, P_2O_5, K_2O is based on Manojlović and Čabilovski, 2020 [41].

Weather conditions during the 2021 and 2022 growing seasons were characterized using temperature and precipitation data obtained from the Rimski Šančevi meteorological station. Observed values were compared with the long-term average for the 1987–2016 period. According to this climatic reference period, the site belongs to a temperate continental, moderately wet, and seasonal climate of the Pannonian Plain (PAN3 zone) [42].

2.5.1. Season 2021

October–March exceeded the long-term average by 27.49 mm, providing favorable soil moisture reserves prior to planting (Figure 1a). April was characterized by above-average precipitation and lower-than-average temperatures, which delayed sowing toward the end of the month but ensured adequate moisture for early crop establishment. Maize plants showed no stress symptoms during early vegetative growth. May received near-average precipitation, which supported uniform vegetative development. The first visible signs of water stress appeared in the second decade of June, when leaf rolling and partial leaf folding were observed, indicating increasing evaporative demand. High air temperatures in late June accelerated soil moisture depletion and prolonged the silking–anthesis interval in both hybrids. July was characterized by significantly above-average temperatures and below-average precipitation, with strong intra-month variability. In the first, second, and third decades of July, temperatures exceeded the long-term average by 2.75 °C, 4.12 °C, and 2.89 °C, respectively, while precipitation deficits ranged from 18.05 to 48.51 mm. On 18 July 2021, a strong storm event accompanied by heavy rainfall and strong wind caused extensive root lodging. Plants that lodged experienced additional stress due to renewed high temperatures and low precipitation following the event. During the month after lodging, total precipitation amounted to only 6 mm, while temperatures remained on average 2.22 °C above the long-term mean. These conditions shortened the grain filling period, reduced kernel filling intensity, and accelerated crop maturation.

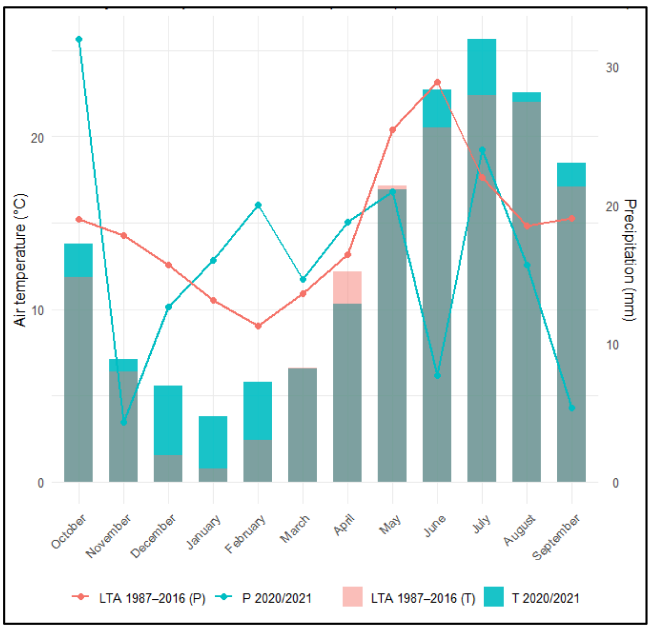

(**a**)

Figure 1. *Cont.*

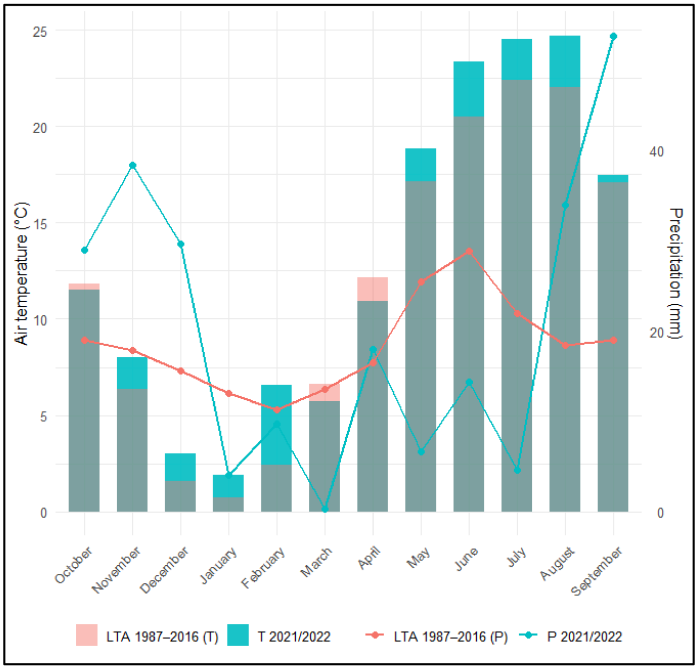

(**b**)

Figure 1. (**a**) Weather conditions in 2020/2021 and long-term average. (**b**) Weather conditions in 2021/2022 and long-term average.

2.5.2. Season 2022

The period from November to March was warmer and wetter than the long-term mean, resulting in favorable soil moisture reserves (Figure 1b). However, spring 2022 began with cooler temperatures and markedly reduced precipitation. From March to May, precipitation was approximately 45% lower than the long-term average. April temperatures were 1.23 °C below the long-term mean, while precipitation was near average and contributed to adequate soil moisture for germination. However, May was extremely dry, with only 3 mm of precipitation during the first two decades, representing a fivefold reduction compared with the long-term average. June and July were characterized by persistent drought and frequent heat waves. Maximum daily air temperatures ranged from 32 °C to 41 °C, while minimum temperatures were consistently above average. Precipitation remained irregular and largely insufficient during this period. Although rainfall increased in late August, these conditions occurred too late to substantially benefit grain filling. Consequently, crop maturation was accelerated, harvest occurred earlier than usual, and grain yield and quality were reduced.

3. Results

The LP showed significant variability, ranging from 0 to nearly 100%, with a high coefficient of variation (CV) (Table 2). It is noteworthy that the lodging observed during the field experiment in 2021 was root lodging, primarily attributed to heavy rainfall and strong winds. In 2022, root lodging was absent, while the lodging that occurred was mainly stalk breakage. Similarly, GY displayed considerable variability, spanning a range of 0.60 to 5.70 t ha^{-1}. The mean GY was 2.66 t ha^{-1}, which was considerably lower than the long-term target yield level of approximately 10 t ha^{-1} used for fertilization planning at the experimental site. This difference indicates that grain yield was not limited by the intended nutrient supply alone but was strongly constrained by seasonal conditions. In both experimental years, spring and summer precipitation was below the long-term mean, while summer temperatures were above the long-term mean (Table 1; Figure 1a,b).

Table 2. Descriptive statistics of maize traits related to yield and lodging susceptibility.

Traits	Min	Max	Mean	SD	CV
LP	0	99.1	18.64	26	139.44
eMOI	0.19	1.05	0.46	0.15	32.21
eSM	0.23	0.83	0.43	0.1	23.87
RT	0.1	0.2	0.14	0.02	12.36
IDmajor	1.96	3.02	2.37	0.19	8.02
IDminor	1.65	2.58	2.08	0.17	8.13
CSA	2.53	5.87	3.83	0.62	16.08
GY	0.6	5.7	2.66	1.22	45.97
KM1000	192.09	303.24	249.63	21.94	8.79
KNE	128.17	621	376.83	83.89	22.26
LAI	1.1	4.9	2.78	0.67	24.2
DW	2.4	8.8	4.75	1.22	25.57
DWUL	0.28	1.11	0.6	0.13	22.12
EL	8.8	18.8	14.45	1.9	13.16
EW	3.5	4.6	4.1	0.21	5.01
RNE	10	19.2	16.08	1.36	8.47
LL	40	87.3	66.24	10	15.09
LW	6.5	11.4	9.26	0.91	9.85
LA	12	31	20.28	3.98	19.64
PW	20.6	74.6	42.07	10.94	26.01
PH	133.9	259.8	195.62	29.04	14.84
EH	35	113.2	76.15	18.16	23.85
EHPH	0.23	0.55	0.39	0.07	17.45
NGL	10.4	16.2	13.04	1.24	9.51
IL	4.2	16.5	8.21	2.47	30.11

LP—lodging percentage; eMOI—the ellipse-based area moment of inertia of the rind in the direction of the minor diameter; eSM—the ellipse-based section modulus in the direction of the minor diameter; RT—rind thickness; IDmajor—the diameter of the maximum axes; IDminor—the diameter of the minimum axes; CSA—cross-sectional area; GY—grain yield; KM1000—the dry mass of 1000 kernels; KNE—kernel number per ear; LAI—leaf area index; DW—internode dry weight; DWUL—dry weight per unit length; EL—ear length; EW—ear width; RNE—kernel rows per ear; LL—leaf length; LW—leaf width; LA—leaf angle; PW—plant width; PH—plant height; EH—ear height; EHPH—ear height/plant height; NGL—the number of green leaves per plant; IL—internode length; Min—minimum value; Max—maximum value; SD—standard deviation; CV—coefficient of variation.

The ellipse-based rind traits (eMOI and eSM) displayed moderate variation, with moderate CV values. In contrast, rind thickness (RT) and ear length (EL) were more stable, with lower CVs. Cross-sectional area (CSA) showed moderate variation. Both stalk diameter traits (IDmajor and IDminor) had low CVs, suggesting uniformity in stalk size across genotypes and treatments. A similar level of uniformity was observed for kernel mass (KM1000), kernel row number (RNE), the number of green leaves (NGL), and leaf width (LW). LW was more consistent than leaf length (LL), despite both traits being measured under the same conditions. Ear width (EW) also showed low variation. Overall, LP and GY showed the greatest variability, whereas stalk dimensions, leaf traits, and kernel traits showed lower variability.

3.1. Holdout Split Validation

As an initial diagnostic analysis, the multi-output neural network was first evaluated using a single random 80/20 train–test split. Hyperparameter sensitivity analysis showed that the 80/20 neural network performance changed across architecture depth and L2 regularization strength (Supplementary Table S1). For GY, the best tested configuration was the 128-64-32 architecture with L2 = 0.20, which achieved RMSE = 0.69 t ha^{-1}, MAE = 0.57 t ha^{-1}, and R^2 = 0.68. The final selected 128-64-32-16 architecture with L2 = 0.20 gave similar but slightly lower GY performance, with RMSE = 0.74 t ha^{-1}, MAE = 0.60 t ha^{-1}, and R^2 = 0.64. For LP, performance was relatively stable across most

configurations, with test R^2 values mostly ranging from 0.89 to 0.92. The final selected model achieved RMSE = 11.48 percentage points, MAE = 7.72 percentage points, and R^2 = 0.92. Because this was a single random split, these results were treated as diagnostic and were compared with repeated cross-validation and year-wise validation.

3.2. Model Comparison Under Repeated Cross-Validation

Repeated five-fold cross-validation showed that predictive performance differed among algorithms and between the two target traits (Table 3). For GY, XGBoost achieved the strongest average performance, with RMSE = 0.80 t ha^{-1}, MAE = 0.64 t ha^{-1}, and R^2 = 0.57. Linear regression, elastic net, and random forest produced similar GY performance, with R^2 values ranging from 0.55 to 0.56. The multi-output neural network had lower average GY performance than the baseline models, with RMSE = 0.86 t ha^{-1}, MAE = 0.70 t ha^{-1}, and R^2 = 0.49. For LP, XGBoost again achieved the strongest average performance, with RMSE = 14.31 percentage points, MAE = 9.44 percentage points, and R^2 = 0.67. The multi-output neural network achieved RMSE = 16.39 percentage points, MAE = 11.04 percentage points, and R^2 = 0.57. Random forest showed similar LP performance to the neural network, with R^2 = 0.56, while linear regression and elastic net were weaker, with R^2 values near 0.49–0.50.

Table 3. Repeated five-fold cross-validation performance of baseline models and multi-output neural network.

Model	Target	RMSE Mean	RMSE 95% CI	MAE Mean	MAE 95% CI	R^2 Mean	R^2 95% CI
XGBoost	GY	0.8	0.78–0.81	0.64	0.62–0.65	0.57	0.55–0.59
Linear	GY	0.81	0.80–0.82	0.68	0.66–0.69	0.56	0.53–0.58
ElasticNet	GY	0.81	0.79–0.83	0.68	0.66–0.69	0.55	0.53–0.57
RandomForest	GY	0.81	0.79–0.83	0.66	0.64–0.68	0.55	0.54–0.57
NN	GY	0.86	0.83–0.89	0.7	0.67–0.73	0.49	0.46–0.53
XGBoost	LP	14.31	13.49–15.13	9.44	8.94–9.94	0.67	0.64–0.70
Linear	LP	17.77	17.21–18.33	13.8	13.36–14.24	0.49	0.45–0.53
ElasticNet	LP	17.76	17.16–18.36	13.82	13.40–14.25	0.5	0.47–0.53
RandomForest	LP	16.76	15.89–17.63	11.84	11.32–12.37	0.56	0.53–0.59
NN	LP	16.39	15.41–17.37	11.04	10.21–11.86	0.57	0.52–0.62

GY—grain yield; LP—lodging percentage; RMSE—root mean square error; MAE—mean absolute error; R^2—coefficient of determination.

Paired comparison showed that the multi-output neural network did not outperform the strongest baseline model. Overall, XGBoost had the strongest predictive performance under repeated cross-validation.

3.3. Year-Wise Validation

Independent year-wise validation showed weak temporal transferability (Table 4). This result should be interpreted in the context of contrasting lodging mechanisms between the two seasons. In 2021, root lodging predominated and was associated with a severe storm event. In 2022, root lodging was absent, while the lodging that occurred was mainly stalk breakage. Because the model target was root lodging percentage, the two years represented strongly different lodging regimes.

When models were trained on 2022 and tested on 2021 data, the training data contained little information about severe root lodging, which limited prediction of the root lodging year. For GY, the best year-wise performance was obtained by elastic net, with R^2 = 0.13, while the multi-output neural network had R^2 = −0.16. For LP, all models had negative R^2 values when tested on 2021 data, with the multi-output neural network achieving R^2 = −0.80. When models were trained on 2021 and tested on 2022 data, GY prediction again remained weak, with the best R^2 value obtained by elastic net (R^2 = 0.10), while the

multi-output neural network had $R^2 = -0.27$. LP transfer to 2022 was especially poor for all models, with strongly negative R^2 values. Because the variance of root lodging percentage was very low in 2022, R^2 became unstable and strongly negative.

Table 4. Independent year-wise validation results.

Test Year	Model	Target	RMSE	MAE	R^2
2021	XGBoost	GY	1.08	0.91	−0.07
2021	Linear	GY	1.31	1.1	−0.58
2021	ElasticNet	GY	0.98	0.78	0.13
2021	RandomForest	GY	1.04	0.85	0
2021	NN	GY	1.13	0.88	−0.16
2021	XGBoost	LP	39.08	26.35	−0.59
2021	Linear	LP	34.02	23.21	−0.21
2021	ElasticNet	LP	37.28	24.93	−0.45
2021	RandomForest	LP	38.39	25.94	−0.54
2021	NN	LP	41.61	28.88	−0.8
2022	XGBoost	GY	1.32	1.13	−0.08
2022	Linear	GY	1.95	1.51	−1.35
2022	ElasticNet	GY	1.21	1.02	0.1
2022	RandomForest	GY	1.37	1.18	−0.16
2022	NN	GY	1.43	1.2	−0.27
2022	XGBoost	LP	45.48	37.69	−30.39
2022	Linear	LP	50.69	45.44	−38
2022	ElasticNet	LP	49.85	44.54	−36.71
2022	RandomForest	LP	42.1	36.92	−25.9
2022	NN	LP	44.74	36.93	−29.38

3.4. Predictor Importance and Trait Associations

Repeated permutation importance with 95% confidence intervals identified EW and RNE as the strongest predictors associated with GY prediction in the multi-output neural network (Figure 2a). Additional predictors with a relatively high mean increase in RMSE included IDmajor, KM1000, KNE, PW, LW, PH, IDminor, NGL and LL. These results indicate that GY prediction was primarily sensitive to ear morphology, kernel-related traits, and several plant architectural traits.

For LP, the highest mean increases in RMSE after permutation were observed for IDmajor, EL and NGL (Figure 2b). Intermediate mean increases in RMSE were observed for RNE, LL, IDminor, PW, LW, EW, LA, KM1000, EHPH, DW, and PH. Smaller effects were observed for IL, EH, and CSA, whereas eSM, DWUL, eMOI, KNE, LAI, and RT showed minimal or near-zero effects. Thus, the highest LP permutation importance values were observed mainly for ear-related, canopy-related, and architectural predictors.

XGBoost SHAP summaries partly support the permutation results while also highlighting differences between modeling approaches. For GY, the highest mean absolute SHAP values were observed for KNE, EL, RT, NGL, PH, DW, EHPH, RNE, DWUL, and LA. For LP, the strongest SHAP contributions were observed for EHPH, IL, EL, LW, RNE, NGL and LA (Table 5).

Repeated permutation importance and XGBoost SHAP identified partly overlapping but not identical predictor rankings. For GY, the strongest agreement between the two interpretability approaches was observed for KNE, RNE, NGL, PH, and EL. This indicates that GY prediction was mainly associated with ear and kernel traits, together with plant height and the number of green leaves.

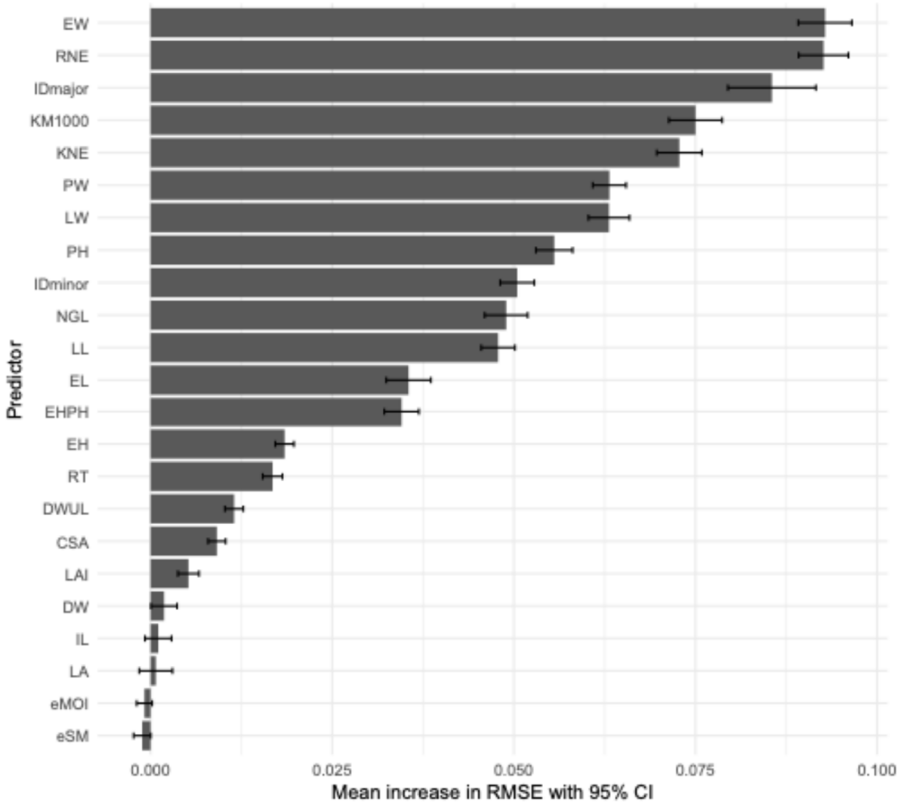

(**a**)

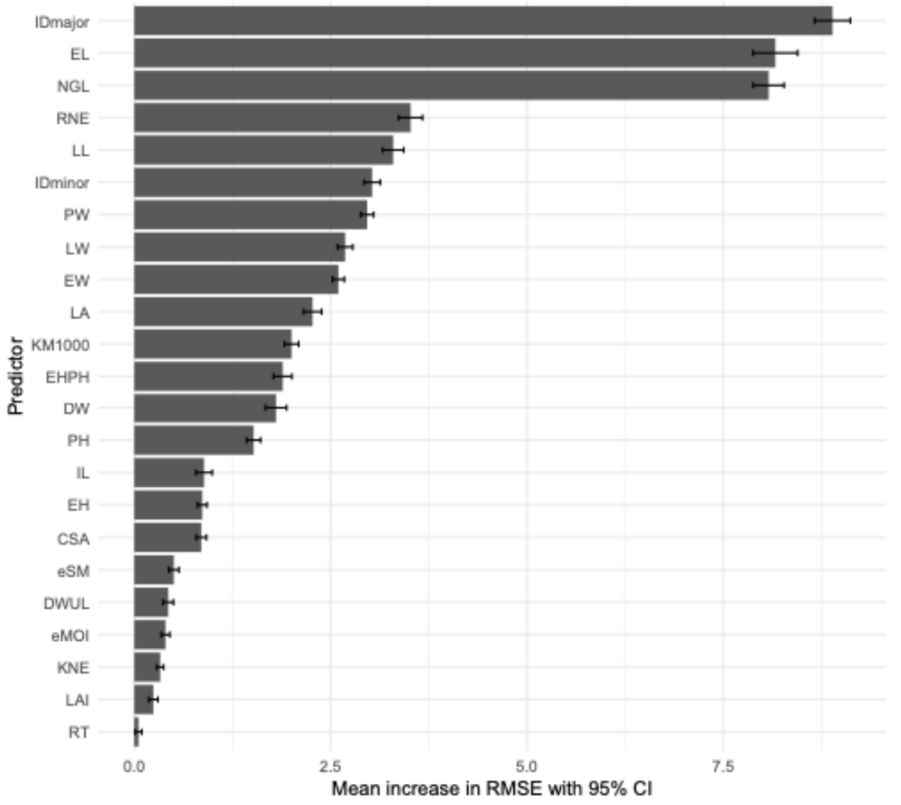

(**b**)

Figure 2. (**a**) Permutation importance stability for grain yield (GY). (**b**) Permutation importance stability for lodging percentage (LP).

Table 5. XGBoost SHAP summaries.

Trait	SHAP for GY	SHAP for LP
KNE	0.44	0.86
EL	0.24	4.27
RT	0.14	0.57
NGL	0.12	1.46
PH	0.11	0.43
DW	0.1	0.62
EHPH	0.09	9.76
RNE	0.08	1.72
DWUL	0.07	0.8
LA	0.06	1.11
LW	0.06	1.92
EH	0.05	0.98
KM1000	0.05	0.22
EW	0.04	0.34
IDmajor	0.04	0.59
LL	0.03	0.59
IDminor	0.03	0.14
eSM	0.02	0.35
CSA	0.02	0.14
IL	0.01	9.06
eMOI	0.01	0.03
LAI	0.01	0.39
PW	0.01	0.46

For LP, the strongest agreement between repeated permutation importance and SHAP was observed for EL, RNE, NGL, LW, LA and EHPH. This indicates that LP prediction was associated with ear size, the number of green leaves, leaf and canopy geometry and vertical plant structure. When the analysis was restricted to the top predictors for each target and each interpretability method, only RNE and NGL were consistently shared between GY and LP across both permutation importance and SHAP. These two traits were therefore interpreted as the most stable shared predictors in the present dataset.

Supplementary ALE plots were used to examine the direction and shape of model-estimated associations for selected high-ranking predictors from the 80/20 neural network model. For GY, ALE diagnostics showed increasing model-estimated effects for EW, RNE, KM1000, KNE, NGL, EL, PH, and EH, while PW, LW, and LL showed decreasing or nonlinear local effects. For LP, increasing model-estimated effects were observed for IDmajor, EL, RNE, LL, LA, KM1000, EHPH, DW, and IL, whereas NGL, PW, LW, EW, PH, and IDminor showed decreasing or nonlinear local effects (Supplementary Figure S1). Among the traits consistently shared between GY and LP across both permutation importance and SHAP, RNE showed increasing ALE effects for both predicted GY and predicted LP. In contrast, NGL showed an increasing ALE effect for predicted GY, but a decreasing or non-linear ALE effect for predicted LP.

4. Discussion

Previous studies have shown that machine learning performance in crop prediction depends strongly on the target trait, predictor set, dataset size, and validation strategy. In maize, XGBoost has been used for GY prediction based on farmer-level production data [43]. Other machine learning approaches, including XGBoost, SVM, k-NN, RF, ANN, LSTM, and RNN, have also been applied to yield or lodging prediction in dry pea, oilseed rape, rice, wheat, tomato, potato, banana, and maize [44–48]. Although these studies differ in crop,

predictor structure, and target trait, they support the same methodological point: model selection should be based on direct comparison rather than on model complexity alone.

The present results support this point. In the initial 80/20 holdout split, the multi-output neural network showed good internal fit, especially for root lodging percentage. However, repeated five-fold cross-validation gave more conservative estimates and showed that XGBoost achieved the strongest average predictive performance for both GY and LP. Cross-validation is one of the most widely used data resampling methods to assess the generalization ability of predictive models [49]. The main value of the multi-output neural network in this dataset was exploratory as it provided a joint framework for examining trait associations shared between grain yield and root lodging. This distinction is important because simultaneous prediction does not automatically imply better prediction, especially when the dataset is small and environment-specific [50].

Year-wise validation represented a stricter test because the model was trained in one season and tested in another. The weak year-wise transferability, especially for LP, shows that root lodging prediction was strongly affected by seasonal conditions and lodging mechanism. This is especially important because root lodging and stalk lodging are not necessarily controlled by the same traits [51]. Although both seasons were unfavorable for high grain yield, they differed in the type of stress imposed on the crop. In 2021, root lodging occurred after a storm event, and the lodged plants were subsequently exposed to high temperatures and limited precipitation during grain filling. In 2022, drought and heat stress dominated the growing season, while root lodging was absent and the observed lodging was mainly stalk breakage. The weak year-wise validation therefore reflects a biological difference between the two seasons.

The role of ethephon should also be considered when interpreting the model estimated trait associations. Ethephon was included as an experimental factor to induce controlled variation in plant architecture and lodging-related traits. Therefore, its influence on traits such as plant height, ear position, internode characteristics and canopy structure was not an uncontrolled source of variation, but part of the experimental design. The identified predictors reflect trait variation generated by the combined effects of hybrid, ethephon rate, sowing density, seasonal conditions, and measured plant morphology. For this reason, the trait associations reported here are interpreted as treatment and environment-specific model-estimated associations rather than direct causal effects.

Traditionally, lodging and grain yield have often been modeled separately, although they are biologically connected traits [52,53]. In wheat, yield-related traits such as spike fertility, grain number per unit area, and harvest index interact with lodging resistance, creating a trade-off between productivity and standability [52]. More tillers can increase yield potential but can also affect lodging risk through changes in stalk strength and root anchorage [54]. The Wheat Yield Consortium also emphasized that modeling optimal trait combinations is one approach for increasing yield while maintaining lodging resistance [55]. Later, the International Wheat Yield Partnership reported that wheat lines with more suitable canopy architecture can improve light management, biomass production, grain set, and lodging resistance [56]. These examples do not directly transfer to maize, but they support the broader concept that yield formation and lodging resistance should be interpreted together. In the present study, GY prediction was primarily sensitive to ear morphology, kernel-related traits, and several plant architectural traits. LP prediction depended more strongly on ear dimensions, vertical plant structure, canopy architecture, and traits associated with above-ground mechanical load than on individual stalk morphology traits alone. However, the overlap of traits between GY and LP became more selective. In the XGBoost SHAP analysis, KNE, EL, NGL, EHPH, RNE, DWUL, and LA were shared between the top ten predictors for both GY and LP. In the neural network

permutation importance analysis, EW, RNE, IDmajor, PW, LW, IDminor, NGL, and LL were shared between the top ten predictors for both traits. However, only two traits, NGL and RNE, were shared between GY and LP across both interpretability approaches. RNE can be interpreted as a reproductive sink and ear structure trait. Its consistent presence across both interpretability approaches suggests that kernel row arrangement helped predict both GY and LP. The ALE diagnostics supported this interpretation, as RNE showed an increasing model-estimated effect for both predicted GY and predicted LP. For GY, this is biologically expected because RNE contributes to kernel number and ear productivity. For LP, higher reproductive sink capacity can be associated with greater ear load and altered above-ground mass distribution, which can influence lodging risk when anchorage and structural support are insufficient. This agrees with previous work showing that lodging resistance and yield formation depend on dry matter allocation between the ear and stem [8]. It also agrees with Xue et al. (2020) [11], who emphasized that maize lodging tolerance should be interpreted together with ear weight, other plant traits, and wind speed. Therefore, RNE should not be interpreted as a direct cause of root lodging, but as a predictor that may capture part of the connection between reproductive development and mechanical loading. The NGL was the second trait consistently shared across both methods. This suggests that the number of green leaves contributed to the joint interpretation of productivity and lodging susceptibility. For GY, this is consistent with the positive ALE pattern and with the role of green leaves in maintaining photosynthetically active canopy area during grain filling. Green leaves are important for carbohydrate supply during kernel development, and a higher green leaf area can support photosynthetic activity and yield formation [57]. For LP, however, the interpretation was more complex. Its ALE pattern for LP was decreasing or nonlinear. This means that the NGL helped the models separate different plant vigor and canopy profiles, but it should not be interpreted as a simple positive driver of root lodging. Larger canopy development can increase shoot biomass and exposure to wind under storm conditions, but the present model suggests that the relationship between the NGL and root lodging depends on its interaction with other canopy, ear, and architectural traits.

Other ear and reproductive traits were important, but their relevance was more method-dependent. KNE was the strongest GY predictor in SHAP and showed a positive ALE pattern for GY, but it was not consistently shared across both interpretability methods for LP. This suggests that KNE was mainly a yield-related predictor in the present dataset. EL showed positive ALE trends for both GY and LP, especially for LP, indicating that the neural network associated longer ears with greater predicted yield and greater predicted root lodging under the observed conditions. EW and KM1000 also showed positive ALE patterns for GY, while KM1000 showed an increasing ALE pattern for LP. These results support the idea that reproductive sink size and ear dimensions contributed to both productivity and mechanical loading, but the exact ranking of these traits depended on the interpretability method.

Vertical architecture traits were more clearly connected with LP than with GY. EHPH and IL were emphasized by SHAP and showed increasing ALE trends for LP. This supports the view that the vertical distribution of plant mass and the position of the ear relative to the stalk affected model-estimated root lodging risk. A higher ear position or longer internode may increase the bending moment on the plant under wind and rainfall, especially when root anchorage is insufficient.

Leaf and canopy geometry traits also contributed to prediction, but their effects were not uniform. LA and LL showed increasing ALE trends for LP, suggesting that leaf angle and leaf length contributed to model-estimated lodging susceptibility. In contrast, LW, PW, and EW showed decreasing or nonlinear ALE patterns for LP. These differences show that canopy architecture cannot be reduced to a single “larger canopy equals higher lodging”

explanation. LW, LA, LL, and PW may influence light interception, canopy load, and wind exposure, but their effects depend on the whole plant architecture and correlated traits. PW is also relevant for maize performance under higher planting density or narrower row environments [58]. However, the present models do not prove that changing PW, LW, LA, or LL would directly reduce root lodging without affecting yield. These traits should be treated as candidate architectural predictors that require validation across additional environments and genotypes.

The idea of increasing kernel number per area rather than kernel number per ear remains agronomically relevant, but it should be treated as a hypothesis rather than a conclusion from the present models. Prolific hybrids may offer one possible way to distribute reproductive load across more ears, but previous studies reported different responses in yield and lodging [59–61]. Therefore, prolificacy, plant density, canopy architecture, and reproductive load distribution should be tested directly before they are recommended as strategies for reducing lodging risk. This is especially important because root lodging and stalk lodging are not necessarily controlled by the same trait complexes [50].

5. Conclusions

This study shows that joint modeling of maize grain yield and root lodging can help identify shared trait associations, but it also shows the limits of using a multi-output neural network on a small, environment-specific dataset. In the initial 80/20 holdout split, the neural network showed good internal fit, especially for root lodging. However, repeated five-fold cross-validation gave more conservative estimates and showed that XGBoost performed better than the multi-output neural network for both GY and LP. Therefore, the repeated cross-validation provides the stronger evidence of predictive performance. The neural network was useful as an exploratory tool, but it did not outperform simpler or more established machine learning models. The results indicate that yield and root lodging were partly linked through ear-related traits, canopy structure, the number of green leaves, and plant architecture. However, the exact ranking of predictors depended on the interpretability method. Traits supported by both neural network permutation importance and XGBoost SHAP should be treated as the most reliable associations. Under the top trait comparison, RNE and NGL were the only traits consistently shared between GY and LP across both interpretability approaches, indicating that reproductive sink structure and green leaf persistence were the clearest shared predictors in this dataset. Year-wise validation showed weak transferability between seasons, mainly because the two years differed strongly in lodging conditions and lodging mechanism. Overall, this study should be viewed as an exploratory framework for joint trait analysis under defined environmental conditions.

Supplementary Materials: The following supporting information can be downloaded at https://www.mdpi.com/article/10.3390/crops6030059/s1: Figure S1: ALE diagnostic plots for the highest ranking predictors from the 80/20 neural network model; Table S1: Hyperparameter sensitivity analysis for the 80/20 neural network model.

Author Contributions: Conceptualization, D.D. and D.S.; methodology, D.D. and D.S.; software, D.D.; validation, D.D.; formal analysis, D.D.; investigation, D.D., A.Đ. and M.T.; visualization, D.D.; supervision, G.B. and B.P. All authors have read and agreed to the published version of the manuscript.

Funding: This research received no external funding.

Data Availability Statement: The raw data supporting the conclusions of this article will be made available by the authors on request.

Acknowledgments: This research was supported by the Ministry of Science, Technological Development and Innovation of the Republic of Serbia, grant number: 451 03 33/2026 03/200032.

Conflicts of Interest: The authors declare no conflict of interest.

References

1. Zhang, R.; Ma, S.; Li, L.; Zhang, M.; Tian, S.; Wang, D.; Liu, K.; Liu, H.; Zhu, W.; Wang, X. Comprehensive utilization of corn starch processing by-products: A review. *Grain Oil Sci. Technol.* **2021**, *4*, 89–107. [CrossRef]
2. Peng, D.; Chen, X.; Yin, Y.; Lu, K.; Yang, W.; Tang, Y.; Wang, Z. Lodging resistance of winter wheat (*Triticum aestivum* L.): Lignin accumulation and its related enzymes activities due to the application of paclobutrazol or gibberellin acid. *Field Crops Res.* **2014**, *157*, 1–7. [CrossRef]
3. Stubbs, C.J.; Oduntan, Y.A.; Keep, T.R.; Noble, S.D.; Robertson, D.J. The effect of plant weight on estimations of stalk lodging resistance. *Plant Methods* **2020**, *16*, 128. [CrossRef] [PubMed]
4. Zheng, M.; Lv, L.; Cui, Y.; Shi, Y.; Zhang, J. Moderate Nitrogen Management Enhancing Maize Lodging Resistance by Reducing Pathogen Infection and Expansion of Stalk Rot. *Agronomy* **2025**, *15*, 787. [CrossRef]
5. Zhu, R.; Ding, Y.; Jiang, C.; Yang, J. Technology of preventing downfall and reducing disaster of maize in mechanical harvest era. *Mod. Agric.* **2020**, *2020*, 15–17.
6. Wang, Q.; Xue, J.; Zhang, G.; Chen, J.; Xie, R.; Ming, B.; Hou, P.; Wang, K.; Li, S. Nitrogen split application can improve the stalk lodging resistance of maize planted at high density. *Agriculture* **2020**, *10*, 364. [CrossRef]
7. Berry, P.M.; Sterling, M.; Spink, J.H.; Baker, C.J.; Sylvester-Bradley, R.; Mooney, S.J.; Tams, A.R.; Ennos, A.R. Understanding and reducing lodging in cereals. *Adv. Agron.* **2004**, *84*, 215–269. [CrossRef]
8. Zhang, P.; Gu, S.; Wang, Y.; Xu, C.; Zhao, Y.; Liu, X.; Wang, P.; Huang, S. The relationships between maize (*Zea mays* L.) lodging resistance and yield formation depend on dry matter allocation to ear and stem. *Crop J.* **2023**, *11*, 258–268. [CrossRef]
9. Lorts, C.M.; Lasky, J.R. Competition × drought interactions change phenotypic plasticity and the direction of selection on *Arabidopsis traits*. *New Phytol.* **2020**, *227*, 1060–1072. [CrossRef] [PubMed]
10. Anderegg, L.D.; Loy, X.; Markham, I.P.; Elmer, C.M.; Hovenden, M.J.; HilleRisLambers, J.; Mayfield, M.M. Aridity drives coordinated trait shifts but not decreased trait variance across the geographic range of eight Australian trees. *New Phytol.* **2021**, *229*, 1375–1387. [PubMed]
11. Xue, J.; Ming, B.; Xie, R.; Wang, K.; Hou, P.; Li, S. Evaluation of maize lodging resistance based on the critical wind speed of stalk breaking during the late growth stage. *Plant Methods* **2020**, *16*, 148. [CrossRef] [PubMed]
12. Shah, A.N.; Tanveer, M.; Abbas, A.; Yildirim, M.; Shah, A.A.; Ahmad, M.I.; Wang, Z.; Sun, W.; Song, Y. Combating dual challenges in maize under high planting density: Stem lodging and kernel abortion. *Front. Plant Sci.* **2021**, *12*, 699085. [CrossRef] [PubMed]
13. Oduntan, Y.; Kunduru, B.; Tabaracci, K.; Mengistie, E.; McDonald, A.G.; Sekhon, R.S.; Robertson, D.J. The effect of structural bending properties versus material bending properties on maize stalk lodging. *Eur. J. Agron.* **2024**, *159*, 127262. [CrossRef]
14. Berry, P.M.; Baker, C.J.; Hatley, D.; Dong, R.; Wang, X.; Blackburn, G.A.; Miao, Y.; Sterling, M.; Whyatt, J.D. Development and application of a model for calculating the risk of stem and root lodging in maize. *Field Crops Res.* **2021**, *262*, 108037. [CrossRef]
15. Dunđerski, D. Dejstvo Etefona na Morfološke Osobine Nadzemnog Dela Kukuruza. Ph.D. Thesis, Poljoprivredni Fakultet, Univerzitet u Novom Sadu, Novi Sad, Serbia, 2024. Available online: https://hdl.handle.net/21.15107/rcub_fiver_4885 (accessed on 10 April 2026).
16. Crook, M.J.; Ennos, A.R. The effect of nitrogen and growth regulators on stem and root characteristics associated with lodging in two cultivars of winter wheat. *J. Exp. Bot.* **1995**, *46*, 931–938. [CrossRef]
17. Wang, Q.; Xue, J.; Chen, J.-L.; Fan, Y.-H.; Zhang, G.-Q.; Xie, R.-Z.; Ming, B.; Hou, P.; Wang, K.-R.; Li, S.-K. Key indicators affecting maize stalk lodging resistance of different growth periods under different sowing dates. *J. Integr. Agric.* **2020**, *19*, 2419–2428. [CrossRef]
18. Zhang, P.; Gu, S.; Wang, Y.; Yang, R.; Yan, Y.; Zhang, S.; Sheng, D.; Cui, T.; Huang, S.; Wang, P. Morphological and mechanical variables associated with lodging in maize (*Zea mays* L.). *Field Crops Res.* **2021**, *269*, 108178. [CrossRef]
19. Wang, W.; Guo, W.; Le, L.; Yu, J.; Wu, Y.; Li, D.; Wang, Y.; Wang, H.; Lu, X.; Qiao, H.; et al. Integration of high-throughput phenotyping, GWAS, and predictive models reveals the genetic architecture of plant height in maize. *Mol. Plant* **2023**, *16*, 354–373. [PubMed]
20. Liu, B.; Liu, Y.; Huang, G.; Jiang, X.; Liang, Y.; Yang, C.; Huang, L. Comparison of yield prediction models and estimation of the relative importance of main agronomic traits affecting rice yield formation in saline-sodic paddy fields. *Eur. J. Agron.* **2023**, *148*, 126870. [CrossRef]
21. Elbasi, E.; Zaki, C.; Topcu, A.E.; Abdelbaki, W.; Zreikat, A.I.; Cina, E.; Shdefat, A.; Saker, L. Crop prediction model using machine learning algorithms. *Appl. Sci.* **2023**, *13*, 9288. [CrossRef]

22. Kwaghtyo, D.K.; Eke, C.I. Smart farming prediction models for precision agriculture: A comprehensive survey. *Artif. Intell. Rev.* **2023**, *56*, 5729–5772.
23. Ahmad Latif, N.; Mohd Nain, F.N.; Ahamed Hassain Malim, N.H.; Abdullah, R.; Abdul Rahim, M.F.; Mohamad, M.N.; Mohamad Fauzi, N.S. Predicting heritability of oil palm breeding using phenotypic traits and machine learning. *Sustainability* **2021**, *13*, 12613. [CrossRef]
24. Xing, Y.; Lv, P.; He, H.; Leng, J.; Yu, H.; Feng, X. Traits expansion and storage of soybean phenotypic data in computer vision-based test. *Front. Plant Sci.* **2022**, *13*, 832592. [CrossRef] [PubMed]
25. Liu, Y.; Nie, C.; Zhang, Z.; Wang, Z.; Ming, B.; Xue, J.; Yang, H.; Xu, H.; Meng, L.; Cui, N.; et al. Evaluating how lodging affects maize yield estimation based on UAV observations. *Front. Plant Sci.* **2023**, *13*, 979103. [CrossRef] [PubMed]
26. Chang, Y.; Latham, J.; Licht, M.; Wang, L. A data-driven crop model for maize yield prediction. *Commun. Biol.* **2023**, *6*, 439. [CrossRef] [PubMed]
27. Baker, C.J.; Sterling, M.; Berry, P. A generalised model of crop lodging. *J. Theor. Biol.* **2014**, *363*, 1–12. [CrossRef] [PubMed]
28. Hostetler, A.N.; Erndwein, L.; Reneau, J.W.; Stager, A.; Tanner, H.G.; Cook, D.; Sparks, E.E. Multiple brace root phenotypes promote anchorage and limit root lodging in maize. *Plant Cell Environ.* **2022**, *45*, 1573–1583. [CrossRef] [PubMed]
29. Zhang, Y.; Wang, Y.; Ye, D.; Wang, W.; Qiu, X.; Duan, L.; Li, Z.; Zhang, M. Ethephon improved stalk strength of maize (*Zea mays* L.) mainly through altering internode morphological traits to modulate mechanical properties under field conditions. *Agronomy* **2019**, *9*, 186. [CrossRef]
30. Zhao, Y.; Lv, Y.; Zhang, S.; Ning, F.; Cao, Y.; Liao, S.; Wang, P.; Huang, S. Shortening internodes near ear: An alternative to raise maize yield. *J. Plant Growth Regul.* **2022**, *41*, 628–638.
31. Bernhard, B.J.; Below, F.E. Plant population and row spacing effects on corn: Plant growth, phenology, and grain yield. *Agron. J.* **2020**, *112*, 2456–2465. [CrossRef]
32. Ritchie, S.W.; Hanway, J.J.; Benson, G.O. *How a Corn Plant Develops*; Iowa State University of Science and Technology, Cooperative Extension Service: Ames, IA, USA, 1986.
33. Cargnelutti Filho, A.; Silveira, D.L.; Alves, B.M.; Carini, F.; Bandeira, C.T.; Pezzini, R.V. Genetic variability and linear relationships between plant architecture and maize grain yield. *Ciência Rural* **2020**, *50*, e20190661. [CrossRef]
34. Heckwolf, S.; Heckwolf, M.; Kaeppler, S.M.; de Leon, N.; Spalding, E.P. Image analysis of anatomical traits in stalk transections of maize and other grasses. *Plant Methods* **2015**, *11*, 26. [CrossRef] [PubMed]
35. Robertson, D.J.; Julias, M.; Lee, S.Y.; Cook, D.D. Maize stalk lodging: Morphological determinants of stalk strength. *Crop Sci.* **2017**, *57*, 926–934. [CrossRef]
36. Novacek, M.J.; Mason, S.C.; Galusha, T.D.; Yaseen, M. Twin rows minimally impact irrigated maize yield, morphology, and lodging. *Agron. J.* **2013**, *105*, 268–276. [CrossRef]
37. IBPGR, C. *Descriptors for Maize*; Consultado 29 de noviembre de 2008; International Maize and Wheat Improvement Center, México City: Mexico, Mexico; International Board for Plant Genetic Resources: Rome, Italy, 1991.
38. Pujianto, U.; Wibawa, A.P.; Akbar, M.I. K-nearest neighbor (k-NN) based missing data imputation. In *2019 5th International Conference on Science in Information Technology (ICSITech)*; IEEE: Piscataway, NJ, USA, 2019; pp. 83–88.
39. Schwertman, N.C.; Owens, M.A.; Adnan, R. A simple more general boxplot method for identifying outliers. *Comput. Stat. Data Anal.* **2004**, *47*, 165–174. [CrossRef]
40. Pavlović, P.; Kostić, N.; Karadžić, B.; Mitrović, M. Soils as Natural Resources. In *The Soils of Serbia*; Springer: Dordrecht, The Netherlands, 2017; pp. 25–29.
41. Manojlović, M.; Čabilovski, R. *Praktikum iz Agrohemije (str. 182)*; Poljoprivredni Fakultet: Novi Sad, Serbia, 2020.
42. Metzger, M.J.; Brus, D.J.; Bunce, R.G.H.; Carey, P.D.; Gonçalves, J.; Honrado, J.P.; Zomer, R. Environmental stratifications as the basis for national, European and global ecological monitoring. *Ecol. Indic.* **2013**, *33*, 26–35. [CrossRef]
43. Sitienei, M.C. Machine Learning in Agriculture with Application in Maize (*Zea mays*) Yield Prediction Modeling in Uasin Gishu County, Kenya. Ph.D. Thesis, University of Eldoret, Eldama Ravine, Kenya, 2024.
44. Bazrafkan, A.; Navasca, H.; Worral, H.; Oduor, P.; Delavarpour, N.; Morales, M.; Bandillo, N.; Flores, P. Predicting lodging severity in dry peas using UAS-mounted RGB, LIDAR, and multispectral sensors. *Remote Sens. Appl. Soc. Environ.* **2024**, *34*, 101157. [CrossRef]
45. Ayalew, A.T.; Lohani, T.K. Prediction of crop yield by support vector machine coupled with deep learning algorithm procedures in Lower Kulfo watershed of Ethiopia. *J. Eng.* **2023**, *2023*, 6675523. [CrossRef]
46. Wang, Q.; Ren, Y.; Wang, H.; Wang, J.; Yang, Y.; Zhang, Q.; Zhou, G. Wind-induced response of rapeseed seedling stage and lodging prediction based on UAV imagery and machine learning methods. *Comput. Electron. Agric.* **2024**, *217*, 108637. [CrossRef]
47. Wilson, A.; Sukumar, R.; Hemalatha, N. Machine learning model for rice yield prediction using KNN regression. *agriRxiv* **2021**. agriRxiv:20210310469. [CrossRef]
48. Rabieyan, E.; Darvishzadeh, R.; Alipour, H. Identification and estimation of lodging in bread wheat genotypes using machine learning predictive algorithms. *Plant Methods* **2023**, *19*, 109. [CrossRef] [PubMed]

49. Bates, S.; Hastie, T.; Tibshirani, R. Cross-validation: What does it estimate and how well does it do it? *arXiv* **2021**, arXiv:2104.00673.
50. Zhang, T.; Jin, C.J.; Song, Y.; Li, D. Are Neural Networks Better than Machine Learning? A Comparative Study for Travel Mode Predictions. *Systems* **2025**, *13*, 1099. [CrossRef]
51. Xue, J.; Gao, S.; Fan, Y.; Li, L.; Ming, B.; Wang, K.; Xie, R.; Hou, P.; Li, S. Traits of plant morphology, stalk mechanical strength, and biomass accumulation in the selection of lodging-resistant maize cultivars. *Eur. J. Agron.* **2020**, *117*, 126073. [CrossRef]
52. Foulkes, M.J.; Slafer, G.A.; Davies, W.J.; Berry, P.M.; Sylvester-Bradley, R.; Martre, P.; Calderini, D.F.; Griffiths, S.; Reynolds, M.P. Raising yield potential of wheat. III. Optimizing partitioning to grain while maintaining lodging resistance. *J. Exp. Bot.* **2011**, *62*, 469–486. [CrossRef] [PubMed]
53. Guo, Z.; Liu, X.; Zhang, B.; Yuan, X.; Xing, Y.; Liu, H.; Luo, L.; Chen, G.; Xiong, L. Genetic analyses of lodging resistance and yield provide insights into post-Green-Revolution breeding in rice. *Plant Biotechnol. J.* **2021**, *19*, 814–829. [PubMed]
54. Murchie, E.H.; Reynolds, M.; Slafer, G.A.; Foulkes, M.J.; Acevedo-Siaca, L.; McAusland, L.; Sharwood, R.; Griffiths, S.; Flavell, R.B.; Gwyn, J.; et al. A 'wiring diagram'for source strength traits impacting wheat yield potential. *J. Exp. Bot.* **2023**, *74*, 72–90. [PubMed]
55. Reynolds, M.; Bonnett, D.; Chapman, S.C.; Furbank, R.T.; Manès, Y.; Mather, D.E.; Parry, M.A. Raising yield potential of wheat. I. Overview of a consortium approach and breeding strategies. *J. Exp. Bot.* **2011**, *62*, 439–452. [PubMed]
56. International Wheat Yield Partnership Optimizing Crop Canopy Architecture to Enhance Yield (IWYP Science Brief No. 15). International Wheat Yield Partnership. 2021. Available online: https://iwyp.org/wp-content/uploads/sites/34/2021/05/AP05-IWYP-Science-Brief-FINAL.pdf (accessed on 12 December 2025).
57. Blancon, J.; Buet, C.; Dubreuil, P.; Tixier, M.H.; Baret, F.; Praud, S. Maize green leaf area index dynamics: Genetic basis of a new secondary trait for grain yield in optimal and drought conditions. *Theor. Appl. Genet.* **2024**, *137*, 68. [CrossRef] [PubMed]
58. Bernhard, B.J.; Below, F.E. Plant population and row spacing effects on corn: Phenotypic traits of positive yield-responsive hybrids. *Agron. J.* **2020**, *112*, 1589–1600.
59. Varga, B.; Svečnjak, Z.; Knežević, M.; Grbeša, D. Performance of prolific and nonprolific maize hybrids under reduced-input and high-input cropping systems. *Field Crops Res.* **2004**, *90*, 203–212.
60. Brotslaw, D.J.; Darrah, L.L.; Zuber, M.S.; Krause, G.F. Effect of prolificacy on grain yield and root and stalk strength in maize. *Crop Sci.* **1988**, *28*, 750–755. [CrossRef]
61. Thomison, P.R.; Jordan, D.M. Plant population effects on corn hybrids differing in ear growth habit and prolificacy. *J. Prod. Agric.* **1995**, *8*, 394–400. [CrossRef]